**Luminescent Materials** | Hot Paper

Expanding Luminescence Horizons in Macropolyhedral Heteroboranes

Jonathan Bould,* Marcel Ehn, Oleg Tok, Dmytro Bavol, Monika Kučeráková, William Clegg, Miroslava Litecká, Kamil Lang, Kaplan Kirakci, and Michael G. S. Londesborough

Abstract: Luminescence is observed in three novel macropolyhedral nineteen- and eighteen-vertex chalcogenaboranes: $Se_2B_{17}H_{17}$ (**1**), $SeB_{17}H_{19}$ (**3**) and $SeB_{18}H_{20}$ (**4**). This led us to the recognition that previously published macropolyhedral heteroborane species might also exhibit luminescence. Thus, the known nineteen- and eighteen-vertex dithiaboranes $S_2B_{17}H_{17}$ (**2**), *n*-$S_2B_{16}H_{16}$ (**5**) and *i*-$S_2B_{16}H_{16}$ (**6**) were synthesised and also found to exhibit a range of luminescent properties. These macropolyhedral species are very different from the previously unique fluorescent binary borane $B_{18}H_{22}$ in terms of their structural architectures, by the presence of borane cluster hetero atoms, and, as in the cases of **5** and **6**, that their synthetic origins are not derived simply through the modification of $B_{18}H_{22}$ itself. They consequently greatly expand the possibilities of finding new luminescent inorganic borane species.
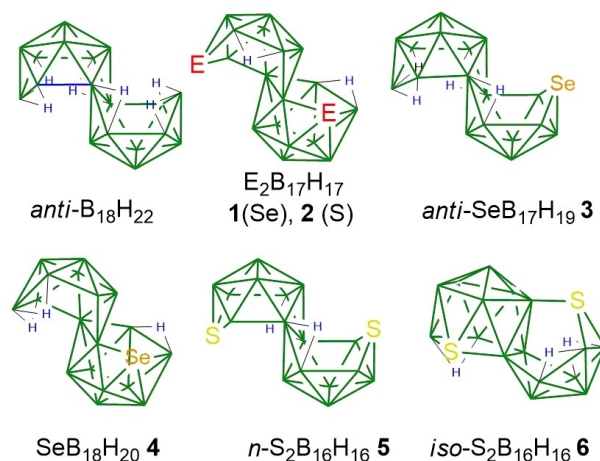
Scheme 1. Schematic structures of the new and known macropolyhedral species described herein. Green vertices are boron atomic positions.

Macropolyhedral boranes can be defined as those compounds in which two or more borane sub-clusters are joined by common boron atoms and in which the multicentre bonding character of boranes extends across the conjunction.[1] The synthesis of the first macropolyhedral binary borane $B_{18}H_{22}$ was reported in the 1960s.[2] The compound comes in two structural isomers, *syn*-$B_{18}H_{22}$ and *anti*-$B_{18}H_{22}$. Solutions of the *anti*-isomer (Scheme 1) exhibit the property of a blue fluorescence emission with a quantum yield of 0.97.[3] A consequence of this is that interest in this

macropolyhedral species has undergone a resurgence due to the recognition that its photostable fluorescence can be used as the gain medium in a borane laser.[4] The photophysical properties of *anti*-$B_{18}H_{22}$ may be modified by the introduction of substituents or ligands to replace the cluster *exo*-terminal hydrogen atoms such as halogens,[5,6,7] alkyl groups,[8] thiol,[9] as well as organo-oxygen and organo–nitrogen substituents.[10] Environmentally sensitive species have been afforded through charge-compensating substituents such as pyridine and isoquinoline,[11] giving molecules capable of thermochromic luminescence,[11a] and the photosensitisation of oxygen.[5] Of all the known binary boranes, *anti*-$B_{18}H_{22}$, and its derivatives, were thought to be the only borane compounds known to have the property of luminescence that are not due to coupling to aromatic substituents such as found in, for example, carborane compounds.[12] This might lead to the conclusion that the fluorescent property of *anti*-$B_{18}H_{22}$, while interesting, is unique to the framework of this particular molecule. However, very recently it has been reported that, similarly to the dithiol derivative 4,4-$(HS)_2$-*anti*-$B_{18}H_{20}$,[9] monothiol and dithiol derivatives of *syn*-$B_{18}H_{22}$ also exhibit luminescence in solution and in the crystalline state.[13] Moreover, it is now recognised that the *syn*-$B_{18}H_{22}$ isomer itself exhibits luminescence in the solid state with a quantum yield of 0.20.[13b]

[*] Dr. J. Bould, Dr. M. Ehn, Dr. O. Tok, D. Bavol, Dr. M. Litecká, Dr. K. Lang, Dr. K. Kirakci, Dr. M. G. S. Londesborough
Institute of Inorganic Chemistry of the Czech Academy of Sciences
Husinec-Řež 250 68, Czech Republic
E-mail: jbould@gmail.com

Dr. M. Kučeráková
Institute of Physics of the Czech Academy of Sciences, Cukrovarnická 10 162 00 Prague 6, Czech Republic

Prof. W. Clegg
Chemistry, School of Natural and Environmental Sciences, Newcastle University, Newcastle upon Tyne NE1 7RU, UK

Angew. Chem. Int. Ed. **2024**, *63*, e202401872 (1 of 7)

© 2024 The Authors. Angewandte Chemie International Edition published by Wiley-VCH GmbH

Nevertheless, these are still octadecaborane species. Here, we report that the occurrence of luminous macropolyhedral species extends well beyond the binary octadecaborane clusters and their substituted derivatives and we now report the syntheses and characterisation of three new substantially different macropolyhedral heteroborane compounds: the new nineteen-vertex selenaborane, $Se_2B_{17}H_{17}$ **1**, which is the selenium analogue of the known $S_2B_{17}H_{17}$ **2**,[14] the eighteen-vertex $SeB_{17}H_{19}$ **3**, and the nineteen-vertex $SeB_{18}H_{20}$ **4**. These new compounds stimulated us to look further into the extensive library of macropolyhedral cluster compounds,[15] and we thus also report herein on the hitherto unrecognised property of luminescence in the known nineteen- and eighteen-vertex thiaboranes, $S_2B_{17}H_{17}$ **2**, n-$S_2B_{16}H_{16}$ **5**, and i-$S_2B_{16}H_{16}$ **6**.[16]

Thus, we are led to anticipate that these new clusters will enable us, through a combination of experimental and quantum chemical computational investigation,[17] to determine the overall structural and electronic properties that lead to luminescent activity over this very diverse set of molecules which have potential to offer utility over a wide range of technologies, including, for example, lasers,[4] sensors,[18] bioimaging,[19] optical data storage,[20] and single-molecule white light emitters.[21]

In this communication we firstly provide a structural characterisation of the new molecules **1**, **3** and **4** that is augmented in the Supporting Information. We subsequently deal with some of the photophysical properties of these new species as well as the other known macropolyhedral heteroborane cluster compounds mentioned above.

$Se_2B_{17}H_{17}$ (1). Low-temperature protonation with concentrated sulphuric acid of dichloromethane solutions of $[Se_2B_{17}H_{18}]^-$,[22] the selenium analogue of the known $[S_2B_{17}H_{18}]^-$,[14] affords $Se_2B_{17}H_{17}$ **1** (see Supporting Information for full experimental details). Compound **1** was characterised by a single-crystal X-ray diffraction study[23] (Figure 1), by multinuclear NMR (Nuclear Magnetic Resonance) spectroscopy (Figures 2, S1, S2 and Table S1), and by mass spectrometry (Figure S3). The cluster compound comprises a *nido*-11-vertex subcluster conjoined with an *arachno*-10-vertex subcluster and is thus very different from the *anti*-octadecaborane species from which its conjugated base is derived,[22] and which contains two identical conjoined *nido*-10-vertex subclusters.

The diselenaborane **1** is structurally very similar to the dithiaborane analogue **2**. However, their chemistries differ somewhat in that, whereas the production of **2** via the acidification of $[S_2B_{17}H_{18}]^-$ proceeds very cleanly, for the diselenaborane, even when the acid is added at low temperature and allowed to warm slowly to ambient temperature, amounts of a minor second component are evident in the boron-11 NMR spectrum. This minor component, compound **3**, is described next. A detailed description of the acidification of both $[S_2B_{17}H_{18}]^-$ and $[Se_2B_{17}H_{18}]^-$, is given in Text S2, Figures S4–6 and Table S2.

Anti-$SeB_{17}H_{19}$ (3). If the addition of acid to the $[Se_2B_{17}H_{18}]^-$ solution is carried out at ambient temperature the minor peaks in the boron NMR spectrum, mentioned above, become predominant and sufficient amounts of this
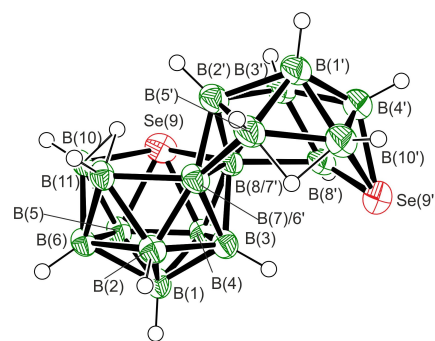

Figure 1. Molecular structure of the nineteen-vertex selenaborane $Se_2B_{17}H_{17}$ (**1**). Displacement ellipsoids for non-hydrogen atoms are drawn at a 50% probability level. The molecule has crystallographic inversion symmetry at the mid-point of the B(7)-B(8) vector; hence the asymmetric unit is half a molecule and the molecule is disordered. Interatomic distances (Å): Se(9)-B(4) 2.097(15), Se(9)-B(5) 2.056(13), Se(9)-B(8) 2.133(16), Se(9)-B(10) 2.141(13), B(5)-B(6) 1.791(15), B(6)-B(7), B(7)-B(8) 1.823(17), B(7)-B(11) 1.910(18). Se(9')-B(4') 1.997(16), Se(9')-B(8') 1.864(17), Se(9')-B(10') 2.031(16), B(5')-B(10') 1.889(18) B(8')-B(8') 2.00(2).
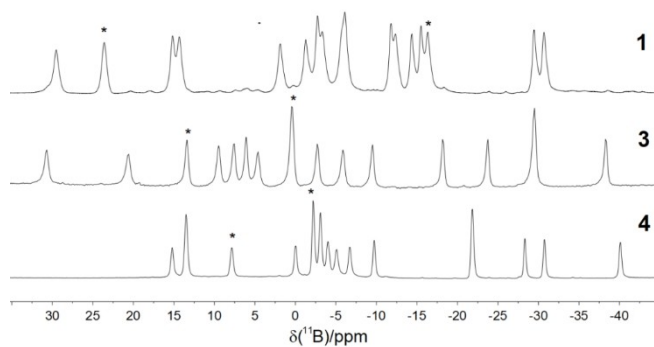

Figure 2. 192.6 MHz ^{11}B-$\{^1$H$\}$ spectra, from top to bottom, of $Se_2B_{17}H_{17}$ (**1**, 293 K), $SeB_{17}H_{19}$ (**3**, 293 K) and $SeB_{18}H_{20}$ (**4**, 331 K) all in $CDCl_3$ solution. Asterisks indicate the positions of singlet resonances in the proton-coupled ^{11}B spectra assigned to the *dicommo* boron vertices linking the subclusters. All other resonances are doublets in the ^{11}B spectra.

species may be isolated by slow vacuum sublimation in an evacuated and flame-sealed NMR tube. Compound **3** has been characterised by multinuclear NMR spectroscopy (Figure 2, Table S3 and Figures S7–8), mass spectrometry (Figure S9) and by a single-crystal X-ray diffraction study[23] (Figure 3 and Scheme 2, Schematic I) as *anti*-$SeB_{17}H_{19}$. The cluster is a structural analogue of *anti*-$B_{18}H_{22}$ in which one $HB(\mu H)_2$ vertex in the octadecaborane species is subrogated by selenium. No thiaborane analogue of this selenaborane is known, although it does resemble the azaborane, *anti*-$NB_{17}H_{20}$ (Scheme 2, schematic II) in which the nitrogen vertex holds a terminal H atom and the formula may be represented as $HNB_{17}H_{19}$.[24] Clearly, the most likely route to this product is by a simple loss of one selenium atom from the $Se_2B_{17}H_{19}$ intermediate formed on initial acidification of $[Se_2B_{17}H_{18}]^-$. We have found that the deposition of selenium
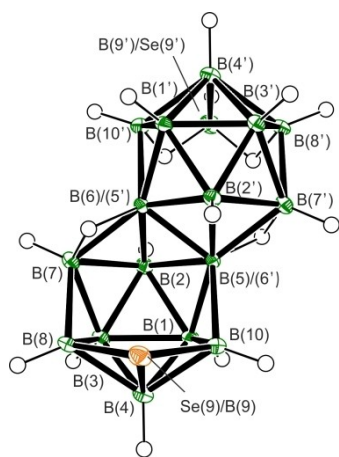
Figure 3. Molecular structure of the eighteen-vertex selenaborane *anti*-SeB$_{17}$H$_{19}$ (**3**). Displacement ellipsoids for non-hydrogen atoms are drawn at a 50% probability level. The molecule has crystallographic inversion symmetry at the mid-point of the B(5)-B(6) vector; hence the asymmetric unit is half a molecule and the molecule is disordered. Interatomic distances (Å): B(5)-B(6), 1.784(4), B(6)-B(2) 1.765(3), B(6)-B(7) 1.816(3), B(7)-B(8) 1.946(3), B(5)-B(10) 1.953(3), Se(9)-B(4) 2.067(3), Se(9)-B(8) 1.983(3), Se(9)-B(10) 1.969(3).
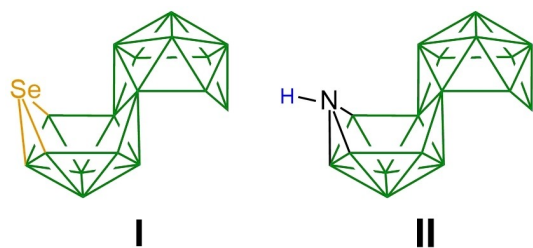
Scheme 2. Schematic structures of heteroatom analogues of *anti*-B$_{18}$H$_{22}$.

is a common complicating feature in working with selena-borane syntheses.

*SeB$_{18}$H$_{20}$ (**4**).* We have previously described the synthesis of anionic 19-vertex [SeB$_{18}$H$_{19}$]$^-$[22] and we therefore examined the addition of concentrated H$_2$SO$_4$ to this compound also. Thus, acidification of pale yellow dichloromethane solutions of the anion, which is prepared from the addition of selenium to [*syn*-B$_{18}$H$_{21}$]$^-$, results in an immediate loss of colour and the formation of a single product as shown from ^{11}B NMR spectroscopy (Figure S10). The compound was characterised as SeB$_{18}$H$_{20}$ (**4**) by a single-crystal X-ray diffraction study[23] (Figure 4), and by multinuclear NMR spectroscopy (Figure 1, Figure S11 and Table S4).

The macropolyhedral cluster **4** comprises a *nido*-11-vertex subcluster conjoined with a *nido*-10-vertex subcluster and may be regarded as the neutral heteroborane analogue of the binary borane anion [B$_{19}$H$_{22}$]$^-$ in which the selenium, Se(9), effectively subrogates the {BH$_2$}$^-$ unit in the binary borane anion[25] (Scheme 3).

Photoluminescence. In the context of the remarkable luminescent properties of *anti*-B$_{18}$H$_{22}$ as described in the Introduction, we were interested to see if similar photo-
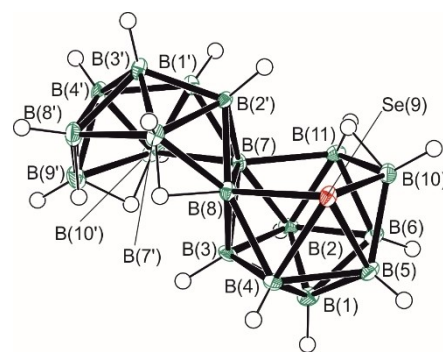

Figure 4. Molecular structure of the nineteen-vertex selenaborane SeB$_{18}$H$_{20}$ (**4**) drawn with 50% probability ellipsoids for non-hydrogen atoms. Interatomic distances (Å) to Se(9): B(4) 2.138(4), B(5) 2.115(4), B(8) 2.183(4), B(10) 2.118(4). B(7)-B(8) 1.824(6), B(7)-B(11) 1.929(5), B(10)-B(11) 1.836(6), B(7)-B(10′) 2.087(6), B(7′)-B(8) 1.932(6), B(7′)-B(10′) 2.087(6). Angles (°): B(8)-Se(9)-B(10) 92.4(1), Se(9)-B(10)-B(11) 115.1(2), B(10)-B(11)-B(7) 109.4(2), Se(9)-B(8)-B(7) 114.6(2), B(11)-B(7)-B(8) 108.1(2). Table S9 lists further interatomic dimensions.
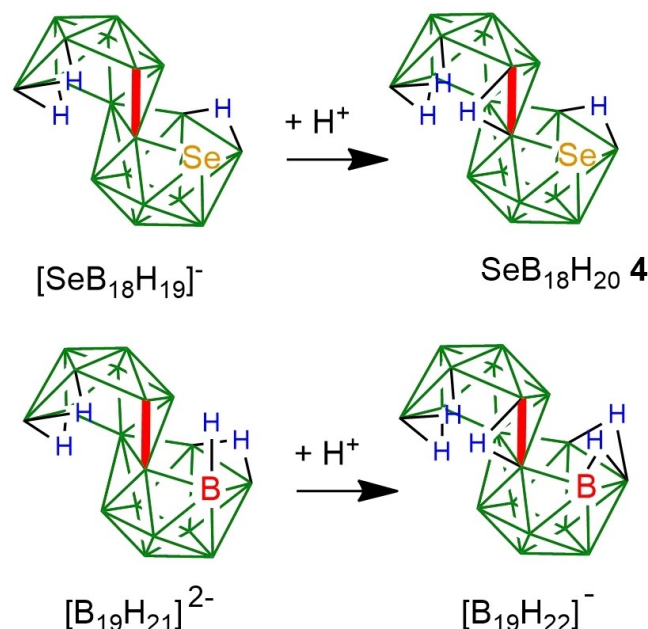
Scheme 3. The protonation of [SeB$_{18}$H$_{19}$]$^-$ and [B$_{19}$H$_{21}$]$^{2-}$ affording SeB$_{18}$H$_{20}$ (**4**) and [B$_{19}$H$_{22}$]$^-$.

activity would be present in the new species that we report here, which are of very different macropolyhedral cluster architecture. Concordantly, we investigated the photophysical properties of the new compounds by means of luminescence spectroscopy and the positive results obtained encouraged us to look further into the properties of similar known macropolyhedral compounds: viz. S$_2$B$_{17}$H$_{17}$ **2**, *n*-S$_2$B$_{16}$H$_{16}$ **5** and *i*-S$_2$B$_{16}$H$_{16}$ **6**. These properties for solid state compounds are summarized in Table 1. Hexane solutions of compounds **1**–**6** generally gave negligible or no measurable luminescence. Only compounds **3** and **5** displayed weak emission in solution. In brief, compound **3** exhibited green

Table 1: Photophysical properties of solids in air atmosphere at room temperature.[a]

Sample	λ_{exc}/nm	λ_L/nm	τ_{air}/μs	Φ_{air}
$Se_2B_{17}H_{17}$ **1**	402	644	22[b]	0.01
$SeB_{17}H_{19}$ **3**	332	628	65[c]	0.13
$SeB_{18}H_{20}$ **4**	387	577	15[c]	< 0.01
$S_2B_{17}H_{17}$ **2**	405	597	9.2×10^3	0.22
n-$S_2B_{16}H_{16}$ **5**	475	567	12[c]	0.05
i-$S_2B_{16}H_{16}$ **6**	407	599	7.9×10^3	0.07

[a] Excitation at the maximum of the excitation spectrum (λ_{exc}); λ_L–emission maximum; τ_{air}–amplitude average luminescence lifetime in air atmosphere; Φ_{air}–luminescence quantum yield in air atmosphere (experimental error of Φ_{air} is ± 0.01); [b] biexponential decay; [c] triexponential decay.

phosphorescence, whereas compound **5** displayed both blue fluorescence and green phosphorescence. Both compounds are singlet oxygen photosensitizers in solution. Nevertheless, our study of these solution-phase properties may be found in the Supporting Information — Table S6, Figure S12 and Text S3. Here, in the manuscript proper, we shall thus consider only the properties of solid state samples of **1–6**.

Upon excitation in the UV/blue region, solid state samples displayed broad emission bands spanning the spectrum from green up to orange region (Figure 5). The absolute emission quantum yields range from < 0.01 for **4** to 0.22 for **2**. Clean NMR spectra were used to verify the purity of the crystalline samples used in all photophysical spectroscopic measurements together with clean HPLC (High Performance Liquid Chromatography) eluted peaks for the more luminescent compounds **2**, **3**, **5** and **6** (see Figures S13–16).

A number of notable points may be made from the observations listed in Table 1:

1) Luminescence has now been found in inorganic macro-polyhedral heteroboranes containing one or two heteroatoms which are not assisted by any organic conjugating substituent groups as found in, for example, Ph-*nido*-$B_{10}H_{13}$.[26]

2) The introduction of Se into *syn*-$B_{18}H_{22}$ retains the luminescence observed in the underlying *syn* cluster isomer,[13b] albeit with a lower quantum yield.

3) Compounds **5** and **6** are not synthesised via macro-polyhedral species as before, but from the fusion of SB_8H_{12} clusters,[16] thus affording a different route to luminescent macropolyhedral heteroboranes.

4) Both **5** and **6** are luminescent but show very different structural characteristics (see Scheme 1) with **5** possessing essentially an *anti*-$B_{18}H_{22}$ architecture with two vertices subrogated by sulphur whereas **6** has conjoined 11-vertex and 8-vertex subclusters, indicating that luminescence in macropolyhedral species is not limited by cluster architecture. Also, in contrast to the *anti*-$B_{18}H_{22}$ analogue, *anti*-$SeB_{17}H_{19}$ **3**, species n-$S_2B_{16}H_{16}$ **5**, *anti*-$B_{18}H_{22}$ analogue, now shows a lower quantum yield than **3**.

5) The 19-vertex $S_2B_{17}H_{17}$ **2** displays the brightest quantum yield of the new species (0.22) and, with a *nido*-11-vertex
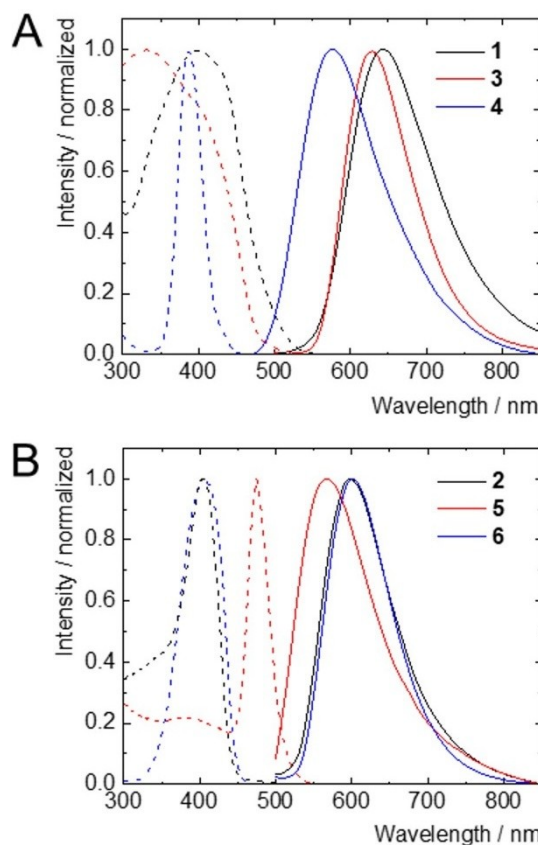

Figure 5. Excitation spectra (dashed lines), recorded at the maximum of emission, and emission spectra (plain lines), excited at the maximum of excitation spectra, of solid samples of the selenium (**A**) and sulphur (**B**) derivatives.

subcluster joined to an *arachno*-10-vertex subcluster, it shows little structural similarity to the double *nido*-10-vertex subcluster architecture of *anti*-$B_{18}H_{22}$.

The structural analogues, compounds **1** and **2**, permit us a direct comparison of the relative effects of selenium and sulphur on the photophysical properties of these species. Here, the sulphur macropolyhedral heteroborane **2** has a luminescence quantum yield twenty times that of its selenium analogue, **1**. Surprisingly, there is a remarkable difference in excited state lifetimes between $E_2B_{17}H_{17}$ compounds **1** and **2**, with the latter sulphur-containing species displaying an extremely long lifetime approaching 10 ms, which is a factor of a thousand times longer than that for selenium analogue **1**. This very long lifetime and the absolute phosphorescence quantum yield of 22 % at room temperature are outstanding for an inorganic phosphor without any heavy atoms/metals.[27] Compound **6**, i-$S_2B_{16}H_{16}$, also records a similarly very long millisecond excited state lifetime.

To unravel the mechanism behind the substantially longer lifetime of compound **2** (and **6**) when compared to the other compounds in this study, which show microsecond lifetimes typical for phosphorescence, we performed measurements of the luminescence properties of **2** in the 100–

300 K range (Figure 6). While no shift of the emission band was observed, its shape, as well as that of the corresponding excitation spectra, revealed a vibrational fine structure at low temperatures. At 100 K the vibronic structure of the emission band was clearly pronounced and the individual vibronic lines were resolved. The luminescence lifetime increases when reducing the temperature, from 9.2 ms at 300 K to 13.1 ms at 100 K (Figure 7), and the luminescence intensity increases to Φ_{air} *ca.* 0.8. These features could be ascribed to the presence of a thermally activated, non-radiative decay channel, which is less effective at low temperatures. Thus, the longer luminescence lifetimes observed for **2** and **6** do not originate from thermally-activated delayed phosphorescence pathways, which would be characterized by a shift of the emission band when varying the temperature,[28] Instead, we suggest that this feature might be attributed to ultra-long-lived excited triplet states, where poor spin-orbit coupling leads to a much lower rate of intersystem crossing ($T_1{\rightarrow}S_0$) and thus, radiative transitions of a highly forbidden character.[29]

In summary, three 19-vertex (**1**, **2**, and **4**) and three 18-vertex heteroboranes (**3**, **5**, and **6**) have been shown to exhibit luminescence. Thus, the work described herein on the study of macropolyhedral heteroborane clusters disrupts any previous possible assumption that luminescence from macropolyhedral borane species might be limited to *anti*-$B_{18}H_{22}$ and its derivatives. As such, our observation and
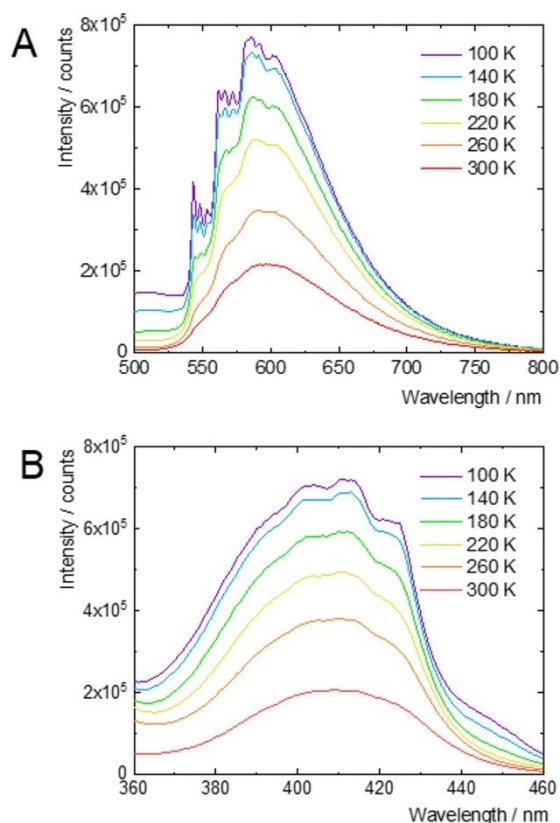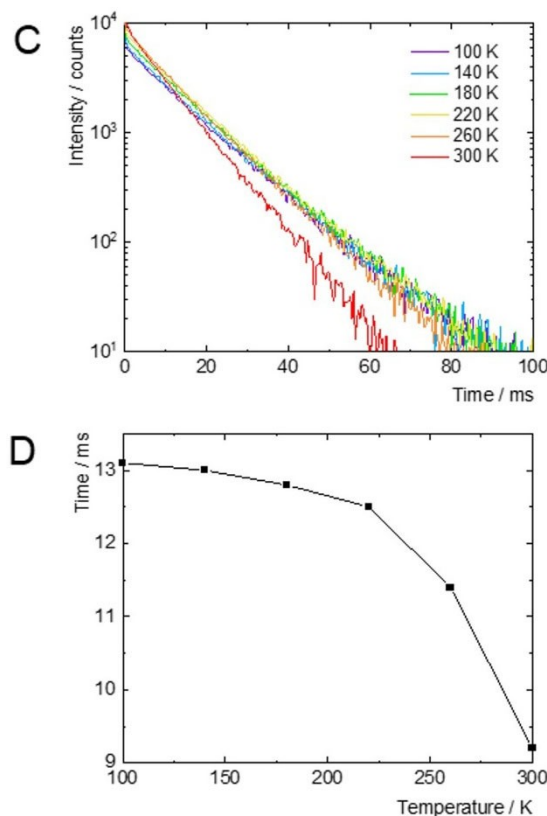

Figure 7. (**C**) Luminescence decay kinetics of solid **2** from 100 to 300 K, excited at 410 nm and recorded at 600 nm (fast decay at the early beginning was due to pulse scattering). (**D**) Temperature dependence of the luminescence lifetime of solid **2** from 100 to 300 K.

study of luminescence in these very different cluster geometries represents a major change in the availability of light conversion from this inorganic molecular class, and opens this new field in photoactive species to far greater horizons.

Supporting Information

The data that support the findings of this study are available in the supplementary material of this article. Additional references are given within the Supporting Information (Ref. [30]).

Acknowledgements

Figure 6. (**A**) Emission spectra of solid **2** from 100 to 300 K, excited at 410 nm. (**B**) Corresponding excitation spectra, recorded at 600 nm.

Conflict of Interest

The authors declare no conflict of interest.

Data Availability Statement

The data that support the findings of this study are available in the supplementary material of this article.

[1] M. A. Beckett, B. Brellochs, I. T. Chizhevsky, T. Damhus, K.-H. Hellwich, J. D. Kennedy, R. Laitinen, W. H. Powell, D. Rabinovich, C. Viñas, A. Yerin, *Pure Appl. Chem.* **2020**, *92*, 355–381.

[2] a) A. R. Pitochelli, M. F. Hawthorne, *J. Am. Chem. Soc.* **1962**, *84*, 3218–3218; b) P. G. Simpson, W. N. Lipscomb, *J. Chem. Phys.* **1963**, *39*, 26–34; c) J. D. Kennedy, *Coord. Chem. Rev.* **2016**, *323*, 71–86.

[3] F. P. Olsen, R. C. Vasavada, M. F. Hawthorne, *J. Am. Chem. Soc.* **1968**, *90*, 3946–3951.

[4] a) L. Cerdán, J. Braborec, I. Garcia-Moreno, A. Costela, M. G. S. Londesborough, *Nat. Commun.* **2015**, *6*, 5958; b) M. G. S. Londesborough, D. Hnyk, J. Bould, L. Serrano-Andrés, V. Sauri, J. M. Oliva, P. Kubát, T. Polivka, K. Lang, *Inorg. Chem.* **2012**, *51*, 1471–1479.

[5] M. G. S. Londesborough, J. Dolanský, J. Bould, J. Braborec, K. Kirakci, K. Lang, I. Císařová, P. Kubát, D. Roca-Sanjuán, A. Francés-Monerris, L. Slušná, E. Noskovičová, D. Lorenc, *Inorg. Chem.* **2019**, *58*, 10248–10259.

[6] K. P. Anderson, A. L. Rheingold, P. I. Djurovich, O. Soman, A. M. Spokoyny, *Polyhedron* **2022**, 116099.

[7] a) K. P. Anderson, M. A. Waddington, G. J. Balaich, J. M. Stauber, N. A. Bernier, J. R. Caram, P. I. Djurovich, A. M. Spokoyny, *Dalton Trans.* **2020**; b) M. Ehn, D. Bavol, J. Bould, V. Strnad, M. Litecká, K. Lang, K. Kirakci, W. Clegg, P. G. Waddell, M. G. S. Londesborough, *Molecules* **2023**, *28*, 4505.

[8] a) M. G. S. Londesborough, K. Lang, W. Clegg, P. G. Waddell, J. Bould, *Inorg. Chem.* **2020**, *59*, 2651–2654; b) J. Bould, K. Lang, K. Kirakci, L. Cerdán, D. Roca-Sanjuán, A. Francés-Monerris, W. Clegg, P. G. Waddell, M. Fuciman, T. Polívka, M. G. S. Londesborough, *Inorg. Chem.* **2020**, *59*, 17058–17070.

[9] V. Sauri, J. M. Oliva, D. Hnyk, J. Bould, J. Braborec, M. Merchan, P. Kubát, I. Císařová, K. Lang, M. G. S. Londesborough, *Inorg. Chem.* **2013**, *52*, 9266–9274.

[10] K. P. Anderson, P. I. Djurovich, V. P. Rubio, A. Liang, A. M. Spokoyny, *Inorg. Chem.* **2022**, *61*, 15051–15057.

[11] a) M. G. S. Londesborough, J. Dolanský, L. Cerdán, K. Lang, T. Jelínek, J. M. Oliva, D. Hnyk, D. Roca-Sanjuán, A. Francés-Monerris, J. Martinčík, M. Nikl, J. D. Kennedy, *Adv. Opt. Mater.* **2017**, *5*, 1600694; b) M. G. S. Londesborough, J. Dolanský, T. Jelínek, J. D. Kennedy, I. Císařová, R. D. Kennedy, D. Roca-Sanjuán, A. Francés-Monerris, K. Lang, W. Clegg, *Dalton Trans.* **2018**, *47*, 1709–1725; c) J. Chen, L. Xiong, L. Zhang, X. Huang, H. Meng, C. Tan, *Chem. Phys. Lett.* **2020**, *747*, 137328.

[12] a) D. K. You, M. Kim, D. Kim, N. Kim, K. M. Lee, *Inorg. Chem.* **2023**, *62*, 10003–10013; b) F. Sun, S. Tan, H.-J. Cao, C.-s. Lu, D. Tu, J. Poater, M. Solà, H. Yan, *J. Am. Chem. Soc.* **2023**, *145*, 3577–3587.

[13] a) M. Ehn, M. Litecká, M. G. S. Londesborough, *Inorg. Chem. Commun.* **2023**, *155*, 111021; b) D. K. Patel, B. S. Sooraj, K.

[14] T. Jelínek, J. D. Kennedy, B. Štíbr, M. Thornton-Pett, *Inorg. Chem. Commun.* **1998**, *1*, 179–181.

[15] a) J. D. Kennedy, in *Boron: The Fifth Element, Vol. 20* (Eds.: D. Hnyk, M. McKee), Springer, Heidelberg, New York, Dordrecht and London, **2015**, pp. 139–180; b) E. D. Jemmis, M. M. Balakrishnarajan, P. D. Pancharatna, *Chem. Rev.* **2002**, *102*, 93–144.

[16] P. K. Dosangh, J. Bould, M. G. S. Londesborough, T. Jelínek, M. Thornton-Pett, B. Štíbr, J. D. Kennedy, *J. Organomet. Chem.* **2003**, *680*, 312–322.

[17] a) L. Cerdán, A. Francés-Monerris, D. Roca-Sanjuán, J. Bould, J. Dolanský, M. Fuciman, M. G. S. Londesborough, *J. Mater. Chem. C* **2020**, *8*, 12806–12818; b) J. M. Oliva, A. Francés-Monerris, D. Roca-Sanjuan, in *Boron: The Fifth Element, Vol. 20* (Eds.: D. Hnyk, M. L. McKee), Springer, Heidelberg, New York, Dordrecht and London, **2015**, pp. 97–119.

[18] Z. Wang, X. Gou, Q. Shi, K. Liu, X. Chang, G. Wang, W. Xu, S. Lin, T. Liu, Y. Fang, *Angew. Chem. Int. Ed. Engl.* **2022**, *61*, e202207619.

[19] a) M. Chaari, Z. Kelemen, D. Choquesillo-Lazarte, N. Gaztelu-mendi, F. Teixidor, C. Viñas, C. Nogués, R. Núñez, *Biomater. Sci.* **2019**, *7*, 5324–5337; b) X. Li, X. Tong, Y. Yin, H. Yan, C. Lu, W. Huang, Q. Zhao, *Chem. Sci.* **2017**, *8*, 5930–5940.

[20] S. Abdallah, R. Mhanna, J. Cabrera-González, R. Núñez, A. Khitous, F. Morlet-Savary, O. Soppera, D.-L. Versace, J.-P. Malval, *Chem. Mater.* **2023**, *35*, 6979–6989.

[21] D. S. Tu, P. Leong, S. Guo, H. Yan, C. S. Lu, Q. Zhao, *Angew. Chem. Int. Ed.* **2017**, *56*, 11370–11374.

[22] J. Bould, M. G. S. Londesborough, M. Litecká, R. Macías, S. L. Shea, T. D. McGrath, W. Clegg, J. D. Kennedy, *Inorg. Chem.* **2022**, *61*, 1899–1917.

[23] Deposition numbers 2271992 (for **1**), 2271993 (for **3**), and 2270782 (for **4**) contain the supplementary crystallographic data for this paper. These data are provided free of charge by the joint Cambridge Crystallographic Data Centre and Fachinformationszentrum Karlsruhe. Access structures service https://www.ccdc.cam.ac.uk/structures.

[24] T. Jelínek, J. D. Kennedy, B. Štíbr, *J. Chem. Soc. Chem. Commun.* **1994**, 677–678.

[25] M. G. S. Londesborough, J. Bould, T. Baše, D. Hnyk, M. Bakardjiev, J. Holub, I. Císařová, J. D. Kennedy, *Inorg. Chem.* **2010**, *49*, 4092–4098.

[26] J. Demel, M. Kloda, K. Lang, K. Škoch, J. Hynek, A. Opravil, M. Novotný, J. Bould, M. Ehn, M. G. S. Londesborough, *J. Org. Chem.* **2022**, *87*, 10034–10043.

[27] D. Tu, S. Cai, C. Fernandez, H. Ma, X. Wang, H. Wang, C. Ma, H. Yan, C. Lu, Z. An, *Angew. Chem. Int. Ed. Engl.* **2019**, *58*, 9129–9133.

[28] C. H. Mak, R. Liu, X. Han, Y. Tang, X. Zou, H.-H. Shen, Y. Meng, G. Zou, H.-Y. Hsu, *Adv. Opt. Mater.* **2020**, *8*, 2001023.

[29] O. Mrózek, M. Gernert, A. Belyaev, M. Mitra, L. Janiak, C. M. Marian, A. Steffen, *Chem. Eur. J.* **2022**, *28*, e202201114.

[30] a) G. M. Sheldrick, *Acta Crystallogr. Sect. A* **2015**, *71*, 3–8; b) G. M. Sheldrick, *Acta Crystallogr. Sect. C* **2015**, *71*, 3–8; c) O. V. Dolomanov, L. J. Bourhis, R. J. Gildea, J. A. K. Howard, H. Puschmann, *J. Appl. Crystallogr.* **2009**, *42*, 339–341; d) V. Petříček, M. Dušek, L. Palatinus, *Z. Kristallogr. Cryst. Mater.* **2014**, *229*, 345–352; e) M. J. Frisch, G. W. Trucks, H. B. Schlegel, G. E. Scuseria, M. A. Robb, J. R. Cheeseman, G. Scalmani, V. Barone, G. A. Petersson, H. Nakatsuji, X. Li, M. Caricato, A. V. Marenich, J. Bloino, B. G. Janesko, R. Gomperts, B. Mennucci, H. P. Hratchian, J. V. Ortiz, A. F. Izmaylov, J. L. Sonnenberg, D. Williams-Young, F. Ding, F. Lipparini, F. Egidi, J. Goings, B. Peng, A. Petrone, T.

Henderson, D. Ranasinghe, V. G. Zakrzewski, J. Gao, N. Rega, G. Zheng, W. Liang, M. Hada, M. Ehara, K. Toyota, R. Fukuda, J. Hasegawa, M. Ishida, T. Nakajima, Y. Honda, O. Kitao, H. Nakai, T. Vreven, K. Throssell, J. J. A. Montgomery, J. E. Peralta, F. Ogliaro, M. J. Bearpark, J. J. Heyd, E. N. Brothers, K. N. Kudin, V. N. Staroverov, T. A. Keith, R. Kobayashi, J. Normand, K. Raghavachari, A. P. Rendell, J. C. Burant, S. S. Iyengar, J. Tomasi, M. Cossi, J. M. Millam, M. Klene, C. Adamo, R. Cammi, J. W. Ochterski, R. L. Martin, K. Morokuma, O. Farkas, J. B. Foresman, D. J. Fox, *Gaussian 16, Revision C.01*, Wallingford CT, **2016**; f) D. L. Ormsby, R. Greatrex, J. D. Kennedy, *Dalton Trans.* **2008**, 1625–1634; g) T. Jelínek, J. D. Kennedy, B. Štíbr, M. Thornton-Pett, *Angew. Chem. Int. Ed. Engl.* **1994**, *33*, 1599–1601; h) Oxford Diffraction/Agilent Technologies UK Ltd, Yarnton, UK, **2020**.